FERMILAB-CONF-06-293-TD

Superconducting Solenoid Magnet Test Results

R. Carcagno, J. Dimarco, S. Feher, C.M. Ginsburg, C. Hess, V.V. Kashikhin, D.F. Orris, Y. Pischalnikov, C. Sylvester, M.A.Tartaglia, I. Terechkine, J.C. Tompkins, T. Wokas

Abstract— **Superconducting solenoid magnets suitable for the room temperature front end of the Fermilab High Intensity Neutrino Source (formerly known as Proton Driver), an 8 GeV superconducting H- linac, have been designed and fabricated at Fermilab, and tested in the Fermilab Magnet Test Facility. We report here results of studies on the first model magnets in this program, including the mechanical properties during fabrication and testing in liquid helium at 4.2 K, quench performance, and magnetic field measurements. We also describe new test facility systems and instrumentation that have been developed to accomplish these tests.**

***Index Terms*—Accelerator Magnet, Magnetic Field, Mechanical Stress, Quench Protection, Superconducting Solenoid**

I. Introduction

Solenoid magnets are under consideration at Fermilab for use as focusing elements in the front end of a high power H^- RF linac that could serve as an 8 GeV High Intensity Neutrino Source (HINS) - previously known as a Proton Driver (PD). The magnetic and mechanical design considerations for these solenoids are challenging: to obtain a high central field (~5T, with ~30% operating margin), with low stray field at adjacent RF cavities, in a short package. They were thoroughly studied and have resulted in a design concept that can be applied to the so-called CH, SS-1 and SS-2 RF sections of the machine [1]. The design requires the use of a superconducting solenoid, with a central “main” coil sandwiched between “bucking” coils at each end; stray flux is further captured by a soft iron yoke surrounding the coils.

In this paper we report on three prototype main solenoidal coil magnets that were built and tested to assess the design, and to confirm the results of modeling predictions for mechanical, quench, and magnetic performance. The three magnets were wound using different superconductor strand, to help evaluate sensitivity of solenoid parameters and performance, and to make a choice of strand to use for a future production stage. They had nearly identical geometry, and there were also small differences in heater arrangement.

Manuscript received August 28, 2006.

Authors are with Fermi National Accelerator Laboratory (FNAL), P.O. Box 500, Batavia, IL 60510. Corresponding author M. A. Tartaglia; phone: (630) 840-3890; e-mail: tartaglia@fnal.gov

FNAL is operated by Universities Research Association Inc. under Contract No. DE-AC02-76CH03000 with the United States Department of Energy

II. Magnet Fabrication

The coil geometry is illustrated in Fig. 1. Three test solenoids, known as PDST01, PDST02, and PDST03, were wound using insulated Cu/NbTi wire under tension of ~20 N around a copper bobbin fitted (with some radial overlap) around a stainless steel (SS-316) beam tube. An additional layer of 50 μm thick fiberglass cloth was added between the (~22) layers of wire. Azimuthal stress in the beam tube was recorded during fabrication and cold testing through the use of two resistive strain gauges mounted on the inner surface of the tube; two unstressed witness gauges were also monitored.

Voltage tap connections were made at the coil edges on selected layers, with finer sampling in the inner high field layers, giving six segments total. In the second magnet, all of the voltage tap connections failed when attempting to use a fine gauge shielded pair conductor; PDST01 and PDST03 used lower gauge (thicker) wires, with no problems.

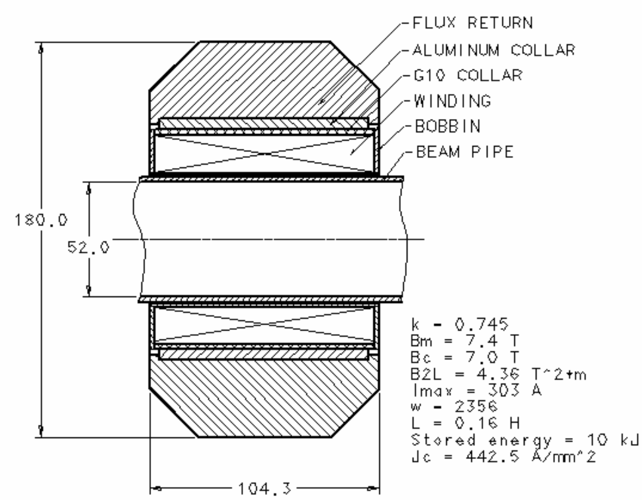

Fig. 1. Cross sectional view of the first Test Solenoid, shown with iron yoke. Dimensions are given in mm.

Four stainless steel quench heaters were installed in each solenoid. All heaters had 50 μm Kapton insulation. In PDST01 and PDST02 the heaters were installed in machined wells in the copper bobbin just under the coil. The well depth was reduced for PDST02 after PDST01 test results suggested a possible air gap causing low thermal conductivity. The PDST03 heaters were installed on the outer surface of the coil.

Each coil package was wrapped with additional fiberglass cloth layers, then vacuum impregnated with epoxy (CDT-101, cured 23 hours at 180 ^{o}F). The outer epoxy material was then machined to the proper final dimension and an aluminum collar with 50 μm radial overlap was added around the coil to apply radial pre-stress to the coil assembly.

III. Test Program Overview

Samples of strands used in each magnet were tested at the Fermilab Technical Division Short Sample Test Facility to parametrize the critical surface for use in modeling the quench performance. Table I lists the major geometrical and superconductor parameters for the three coils.

After fabrication the solenoids were tested [2] in the Fermilab Magnet Test Facility using a modified small vertical dewar test stand [3]. The top plate assembly was outfitted with 300 A, and later 500 A, vapor cooled current leads, and the solenoid was centered around a warm bore anti-cryostat for magnetic measurements. The existing precision VME-based instrumentation and PLC-based controls systems recorded test stand and magnet process variables continuously. The first magnet test was integral to commissioning the new NI/Labview-based systems set up for powering, quench protection, and magnetic measurements of these small magnets. PDST01 was first tested as a bare coil in two thermal cycles, then again with the outer soft iron yoke attached. PDST02 and PDST03 non-yoked coils were each tested in a single cold test, within a week of construction; the tests lasted 1-2 days and used 1000 to 1500 liters of liquid helium.

TABLE I
Test Solenoid Parameters

Quantity	PDST01	PDST02	PDST03
Outer Diameter	93.2 mm	92.7 mm	93.7 mm
N turns	2356	2340	2000
N layers	20	24	22
Packing Factor	0.746	0.754	0.734
Strand Origin	SSC (round)	SSC (flattened)	Oxford (rectang.)
Bare Strand Size	0.808 mm diam	0.99 mm x 0.56 mm	1.02 mm x 0.60 mm
NbTi Filaments	8000 @ 6 μm	8000 @ 6 μm	54 @ 70 μm
Cu/non-Cu	1.5	1.5	1.35

IV. Mechanical Performance

During winding of the coils, the observed buildup of stress differed with the strain gauge azimuth (90 deg. apart); a plausible conjecture posits a slight ellipticity in the pipes. The gauges showed stress increase of at least 35 MPa, compared to the 100 MPa expected from a simplified 2D model [4] used to guide the design. All three coils behaved quantitatively the same: increase of stress during cool down was measured to be about 70 MPa, and stress decreased linearly with current squared, due to Lorentz forces; the stress released during excitation corresponds to about 30 MPa, while the model predicts about 100 MPa. Most importantly, the test data demonstrate clearly that the applied pre-stress is sufficient to prevent coil separation from the bobbin at high current.

V. Quench Protection Studies

A. Quench Protection Overview

Quench protection studies were conducted using a newly developed system [5] in which the quench protection logic is programmed with Labview and runs in a National Instruments FPGA module, using a PXI chassis and controller, and fast sampling ADCs. Three linked applications allow flexible control of the power supply, the quench detection elements, protection heaters and energy extraction circuit, and data capture for quench characterization.

The magnet current was generated by four 125 A Lakeshore (Model 612) power supplies, controlled and measured by a Danfysik (Ultrastab 860) controller and transductor. The analog transductor output was also distributed to the magnetic measurement and VME/unix data acquisition systems. For operation above 100 A, a diode was installed in parallel with the solenoid as a precaution to protect the power supplies from possible large voltage transients. (This limited bipolar magnetic hysteresis measurements to low current.)

B. Heater Protection Studies

Before quench training, we explored the ability of the quench heaters to initiate a quench for magnet protection [2, 6]. The quench delay from heater firing to onset of resistive voltage growth was measured as a function of heater power supply voltage at different solenoid operating currents. Internally a parallel electrical connection was made of two pairs of heaters wired in series. The heater power supply was operated at its minimum capacitance (2.4 mF); its minimum charging voltage was 58 V, so to extend the dynamic range of energy deposition a resistor was installed in parallel with the magnet heaters, roughly halving the load resistance. The discharging heater pulses were exponential with the expected time constant (6 to 8 ms). Fig. 2 illustrates the behavior of quench onset delay for PDST02; the PDST03 profile is quite similar. The model successfully predicts the 300 A delay.

From study of voltage tap signals captured during the heater tests, it was clear that the PDST01 (PDST03) quenches started in the inner (outer) layers, i.e., those closest to the heaters. Because the dump resistor was switched into the

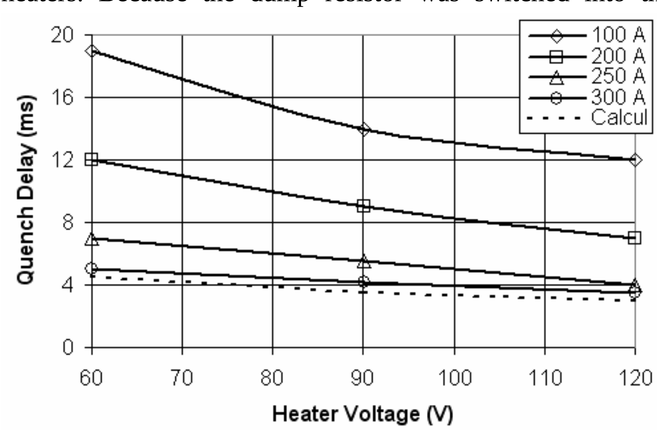

Fig. 2. Delay of quench onset as a function of heater voltage at constant solenoid currents from 100 A to 300 A, for PDST02. The model prediction is shown (dashed line) for the 300 A case.

circuit at quench detection time, quench propagation to other layers was not observed. (This was studied further in the solenoid survival test.) Since spontaneous quenches are expected to originate primarily in the high field inner coil region, the outer coil heaters can be used to quickly initiate quenches there (very low field region) with short delay.

C. Quench Training

Each magnet was trained by ramping to quench at low ramp rate (1 or 2 A/s) until a quench current plateau was reached. Protection heaters and external dump resistor were used to dissipate the stored energy during training. Training and ramp rate dependence are illustrated in Fig. 3. All three magnets trained quickly, and ramp rate dependence was weak. (They are not required to ramp quickly in HINS). Magnet PDST01 did not retrain after a thermal cycle.

A comparison is shown in Table II of the maximum measured quench current with the prediction from model: they are all consistent within about 1-2%. The iron yoke concentrates the flux and leads to a higher coil field, which results in the lower quench current seen in the table.

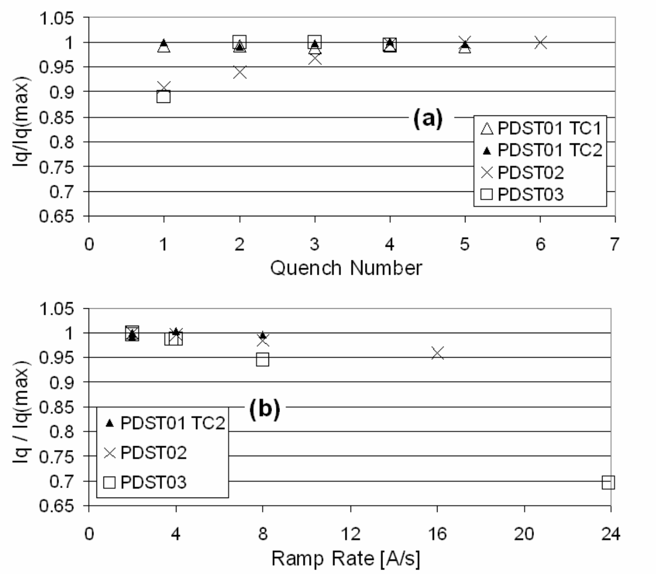

Fig. 3. Quench Training History (a) and Ramp Rate Dependence (b) for three test solenoids, relative to the maximum quench current for each. All training events were well above the nominal solenoid operating point at 0.7.

D. DC Energy Deposition

A significant operating current margin, of order 30%, was desired in this design, to accommodate potentially large heat loads from beam losses. In the tests we measured the amount of heat that could be tolerated at several fixed solenoid currents by putting a DC current through the heaters, and slowly increasing that current until a quench occurred. PDST01 and PDST02 were studied, PDST03 (with different, outer heaters) was not. Table III summarizes these data.

Beam energy loss and temperature distributions will probably differ somewhat from those in this heater test. Also, not all of the heat propagates toward the coil, and the temperature profile in the solenoid is unknown without some modeling. Nevertheless, these data give some indication of the heat loads the solenoid can tolerate: about 2 W at operating current.

TABLE II
TEST SOLENOID PERFORMANCE

Quantity	PDST01 No Yoke (Yoke)	PDST02 No Yoke	PDST03 No Yoke
Quench Current Predicted (A)	304.0 (288.1)	310.0	360.2
Quench Current Measured (A)	307 (292)	311.2	359.6
Central Field Bc at Quench (T)	7.1 (7.26)	7.14	7.07
Max Coil Field at Quench (T)	7.5 (7.67)	7.53	7.47
Peak Transfer Fn Predicted (G/A)	231.5 (250.0)	231.5	197.3
Peak Transfer Fn Measured (G/A)	233.6 (253.5)	234.2	200.5

TABLE III
DC HEATING QUENCH SUMMARY

Solenoid Current (A)	PDST01	PDST02
200	2.8 W	----
250	1.4 W	1.2 W
300	----	0.25 W

E. Solenoid Survival Test

As the last step in the test plan, a test was made to see if the solenoids could absorb the full stored energy (8 to 10 kJ) at the trained quench current. Heater firing was disabled, the external dump resistor switch was delayed 300 ms, and the solenoid was ramped to quench. Solenoids PDST01 and PDST03 survived multiple full energy absorption events with no degradation of subsequent quench performance. PDST02 survival was not tested, given that the conductor quench development properties are not expected to differ from PDST01. The solenoids are robust and can be considered self-protecting.

TABLE IV
QUENCH PROPAGATION DELAYS (MS)

COIL TURNS	PDST01	PDST03	MODEL
1-2	0	0	0
3-4	3	2.5	--
5-6	7	5	--
7-10	25	14	12
11-14	40	23	--
15-20	--	40	44

Without the complication introduced by heaters and the dump resistor, study of the full quench development (up to 300 ms) from voltage tap signals is possible with these quench events. The analysis is slightly complicated by inductive voltages caused by the power supply ramping down after quench detection. The time (in ms) at which resistive voltage growth is detected at each layer are shown in Table IV for PDST01 and PDST03, along with predicted times from the quench development model [7,8]. The propagation in the Oxford strand is slightly faster than in the SSC strand; the model was tuned to reflect the Oxford strand case and examined the time for a quench to propagate through the first half and the whole coil.

VI. Magnetic Measurements

Magnetic field measurements of the test solenoids were made primarily to validate the model predictions and begin to investigate measurement issues in general. Field quality is not an issue, but strength and alignment are. Alignment studies were not possible here, but future tests are planned.

The axial magnetic field strength was measured along the axis of the test solenoids using a one-axis Hall probe (LPT-141-7s) and Group3 Digital Teslameter (DTM-141) with 3 T range. The probe was mounted in a stainless steel tube sized to be a close fit within the warm bore and centered on the solenoid axis. This tube was mounted on a motion stage to provide vertical motion along the solenoid axis, with digital position readout (~0.2 mm precision and reproducibility). During cold testing, the inner warm bore temperature was stable at about 18 ^{o}C.

Measurements were taken both warm (300 K) and cold (4.2 K) for all the bare solenoids and with the iron flux return around PDST01. These included strength versus axial position, central field strength and transfer function, bipolar and unipolar hysteresis loops. For warm tests a Kepko trim current source with precision shunt readout was used to power the solenoid. Unexpected behavior of the magnetic strength at low current led to the discovery and removal of some ferromagnetic material in the probe support after the first solenoid test.

There is nice agreement between predicted and measured strength profiles, normalized to the central field, as shown in

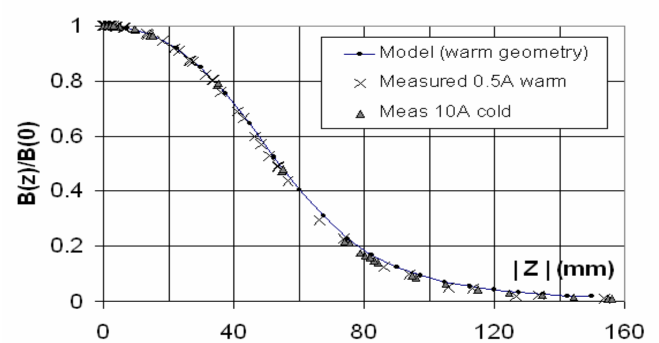

Fig. 4. Comparison of calculated and measured (at 300 K and 4.2 K) axial magnetic field profiles along the central axis of the test solenoid with iron yoke flux return attached. Negative positions are reflected to positive Z.

Fig. 4. In Table II the predicted central and peak magnetic field strengths were given, evaluated at the quench current, along with the predicted and measured solenoid transfer functions (Bc/I). Measured values are about 1.5% above the prediction. Hall probe and current readout calibrations are in progress to establish measurement accuracy at the 0.1% level. Future work will include 3-D field mapping aimed at precisely locating the solenoid axis, and at measuring and shielding small fringe fields outside (at RF cavity surface locations).

Hysteresis studies were conducted to evaluate residual superconductor magnetization fields that might also affect nearby RF cavities, and possibly define criteria for selecting the strand to produce HINS focusing solenoids. Synchronizing field and current measurements during ramping was problematic, so data were captured on (uni-polar) stair-step plateaus, during up and down ramps to various target currents. Fig. 5 shows the hysteresis widths for PDST03 (PDST02 looks similar): the magnetization is complex – resulting from a superposition of many strands in different states - and depends on the ramp history as well as strand properties. Efforts to model this behavior and predict neighboring stray fields are in progress [9].

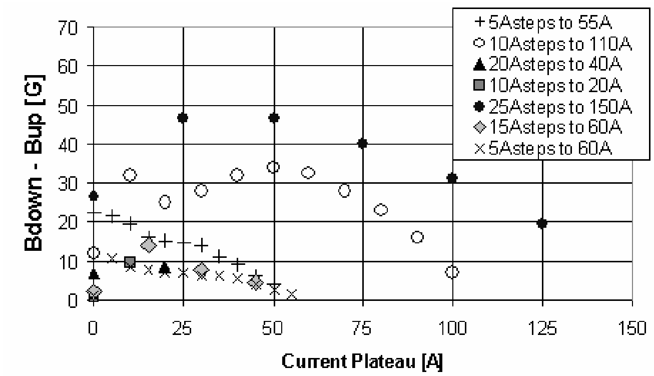

Fig. 5. PDST03 hysteresis width versus current plateau, from stair-step loops (listed in chronological order).

VII. Conclusion

Fabrication and tests of three 7 T solenoid coils were successfully completed. Results confirmed the underlying model predictions, solidifying the design basis for proceeding with the next phase of HINS focusing solenoid development.

Acknowledgment

The authors wish to thank the Fermilab Technical Division Test and Instrumentation Department staff for their dedicated efforts and support of this test program.

References

[1] G.Davis *et al*., “Designing Focusing Solenoids for Superconducting RF Accelerators,” ASC-06, report 5LG03, to be published.

[2] R. Carcagno *et al*., “Test solenoids: expected performance and test results,” TD-06-027, TD-06-028, and TD-06-029, FNAL, July 2006.

[3] R.Rabehl *et al*., “New Facility For Testing LHC HTS Power Leads,” IEEE Trans. Appl. Supercond. v.15, no.2, p.68-3796 (June 2005)

[4] I.Terechkine, “Analysis of Stress in PD Front End Solenoids,” TD-05-039, FNAL, September 2005.

[5] R. Carcagno *et al*., "An FPGA-based Quench Detection and Protection System for Superconducting Accelerator Magnets," Particle Accelerator Conference (PAC 05), Knoxville, Tennessee, 16-20 May 2005.

[6] I.Terechkine, “Solenoid Quench Heaters,” TD-06-006, FNAL, February 2006.

[7] P. Bauer and I. Terechkine, “Proton driver front end focusing solenoid quench protection studies. Part 1: Method description and the first iteration,” TD-06-003, FNAL, January, 2006.

[8] I. Terechkine, “Proton driver front end focusing solenoid quench protection studies. Part 2: Test solenoid quench protection,” TD-06-003, FNAL, January, 2006.

[9] V.V. Kashikhin and I. Terechkine, “Solenoid Residual Magnetization Study,” TD-06-040, FNAL, August 2006.